

A Two-Dimensional (z-θ) Fluid/PIC Simulation of Coaxial Hall Thrusters

IEPC-2005-197

*Presented at the 29th International Electric Propulsion Conference, Princeton University,
October 31 – November 4, 2005*

Eduardo Fernandez^{*}
Eckerd College, St. Petersburg, FL 33711

Aaron Knoll[†] and Mark Cappelli[‡]
Stanford University, Stanford, CA 94305

and

Tarik Kaya[§]
Carleton University, Ottawa, ON K1S 5B6, Canada

This paper describes a 2-dimensional simulation of a coaxial Hall thruster that was developed in the axial-azimuthal ($z - \theta$) computational space. Most computational studies of closed-drift Hall accelerators have been in one dimension (1D) along the axial direction or in two dimensions (2D) in the axial and radial dimensions. These 1D and 2D models have had reasonable success in describing the overall behavior of the plasma discharge. However, in these descriptions, the axial transport of electrons is modeled in an ad hoc fashion, usually with a prescribed cross-field mobility. The cross-field electron mobility is likely to be influenced/established by the azimuthal dynamics. Azimuthal perturbations arise from the established equilibrium and, if properly correlated, result in a net axial transport of electrons. The numerical model developed in this study self-consistently evolves the azimuthal electron drifts, and makes no use of ad hoc transport models. Preliminary analysis of the results indicates that azimuthal plasma instabilities do contribute to the axial electron transport process. However, both numerical and theoretical challenges still need to be addressed as there were notable discrepancies in terms of the time averaged ion velocity and electron density characteristics as compared with experimental findings. These differences are partly attributed to spurious “spikes” in the plasma potential, the origins of which are yet to be identified.

Nomenclature

B	= magnetic induction vector
\bar{c}_e	= mean thermal speed of electron
D_{\perp}	= perpendicular electron diffusion coefficient
e	= electron charge
E	= electric field strength
k	= Boltzmann constant
m_e	= electron mass

* Assistant Professor, Natural Sciences Department, fernane@eckerd.edu

† Research Assistant, Mechanical Engineering Department, aknoll@stanford.edu

‡ Professor, Mechanical Engineering Department, cap@stanford.edu

§ Associate Professor, Mechanical and Aerospace Engineering Department, tkaya@mae.carleton.ca

n_s	= number density of species s ($= e, i, n$)
r	= radial displacement
T_e	= electron temperature
\mathbf{u}_e	= electron fluid velocity
\mathbf{v}_i	= ion particle velocity
v	= electron – neutral collision frequency
z	= axial displacement
ϵ_0	= permittivity of free space
μ_\perp	= perpendicular electron mobility
θ	= azimuthal displacement
ϕ	= plasma potential
$\phi_{\text{discharge}}$	= discharge voltage
ϕ^*	= thermalized potential
σ_{en}	= electron-neutral collision cross section
ω_{pe}	= electron plasma frequency
ω_c	= electron cyclotron frequency

I. Introduction

Hall thrusters are an electric propulsion technology that has attracted considerable interest concomitant with the increased number of government and commercial satellites in orbit.¹ The main use of these relatively low power, high I_{sp} rockets lies in low thrust applications such as orbit transfer and orbit station keeping. In Hall thruster plasmas, electrons emitted from a cathode, migrate towards the anode at the base of the discharge channel, and ionize xenon neutrals upon collision. The resulting ions are accelerated out of the device by the electric potential drop between the cathode and the anode, typically a few hundred volts. Such a potential drop is localized near the exit of the device by an external radial magnetic field. While the overall operation of these thrusters is reasonably understood, key physics issues remain open for investigation. Of particular interest is the study of electron transport across the applied magnetic field. It is well known that the electron conductivity in the Hall thruster is much larger than can be inferred from classical collisions alone.² Turbulent fluctuations and wall effects are believed to have a major effect on the local cross-field transport, which, in turn, affects the local electric field, ionization and acceleration of the ions, thrust, and overall discharge behavior. A good understanding of the processes involved in determining this anomalous transport remains the subject of important research not only in regard to Hall thruster plasmas but fusion and astrophysical plasmas as well.

This paper describes our recent development of a numerical simulation of a Hall thruster that was developed in the axial-azimuthal (z - θ) coordinate plane. This model is based on our previous experience in formulating a z - r hybrid particle-in-cell (PIC) model, as described in Fernandez, Cappelli, and Mahesh³.

With the exception of the work by Hirakawa,⁴ and Adams et al.,⁵ prior computational work on Hall thrusters has been one dimensional (1D) in the axial (z) direction or two dimensional (2D) in the axial and radial (r) directions. These prior studies have had reasonable success in describing the overall behavior of the plasma discharge. Most notably, they capture the dominant instability in these devices, the so-called “breathing mode” instability. However missing in these descriptions is the azimuthal electron dynamics. Besides drifting axially along z , opposite to the electric field, electrons in the thruster drift azimuthally as a result of the imposed crossed ($\mathbf{E} \times \mathbf{B}$) electric and magnetic fields. Azimuthal perturbations arise from the established equilibrium and, if properly correlated, result in a net axial transport of electrons.⁶ This effect is not captured in z - r descriptions and the anomalous axial cross-field transport needs to be modeled. Most 2D studies have used a Bohm mobility given by

$$\mu_\perp = \frac{1}{16B} \quad (1)$$

as a model for the electron mobility across the magnetic field.³ Others have used a Bohm-type scaling with B for the mobility with a constant other than 1/16, in order to better fit experiments.⁷ Nonetheless, many plasma transport experiments have demonstrated that electron transport can vary greatly and does not always conform to a Bohm scaling. A recent measurement of electron mobility in Hall discharge channel has revealed that such transport is a complicated function of axial location as well as operating parameters.⁸ In particular, at high voltage, Bohm

transport seems to fare well in the middle of the channel while near the channel exit the transport is reduced to near its classical value, and beyond the channel exit, it appears to be anomalous again. It is apparent from this study that a single model does not properly describe the full plasma region from the anode to the near plume. The use of this experimental spatially-varying mobility in 2D simulations reproduces the measured plasma properties reasonably well,⁹ and such a model has been used to predict the erosion history of the channel walls.¹⁰ However, this mobility applies only to the discharge geometry and conditions for which it was measured, and it is not expected to apply to other thrusters. The lack of a transport model for simulating changing geometries and changing operating conditions severely limits the flexibility and usefulness of these 2D simulations. Reliable Hall thruster simulations are a vital step toward developing and implementing Hall thruster technology, both to support laboratory experiments and to reliably predict the thruster performance in space applications.

As our main motivation, our objectives for this paper are to construct a $z - \theta$ model which self-consistently evolves the azimuthal drifts and makes no use of transport parameters. This is to be contrasted with $z - r$ models, many of which are based on the original model of Fife.¹¹ A schematic of the computational space for the $z - r$ and $z - \theta$ model is provided in the illustration in Fig. 1 and Fig. 2 respectively. It is hoped that the $z - \theta$ simulations can capture high frequency azimuthally-propagating instabilities, and in doing so account for the anomalous axial transport of electrons. Like our past $z - r$ simulation, this $z - \theta$ simulation uses a hybrid fluid/particle-in-cell (PIC) description with the electrons treated as a fluid, and the ions and neutrals treated as discrete particles.

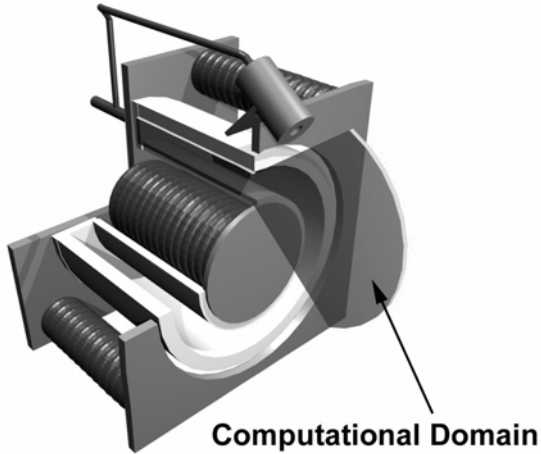


Figure 1: Traditional $z - r$ Computational Plane

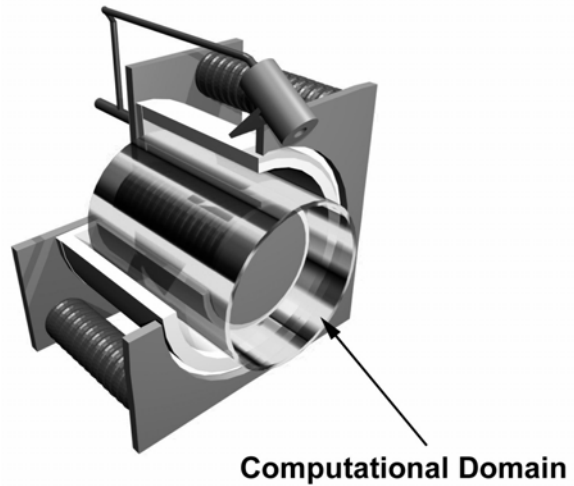


Figure 2: Alternative $z - \theta$ Computational Plane

As described in more detail below, the simulation was run for a number of different operating conditions tested in the laboratory. The preliminary results of this study indicate that the simulation was able to capture high frequency plasma oscillations that resemble experimental observations of emission fluctuations seen using high speed streak photography.¹² Despite the qualitative success of these preliminary calculations, the time averaged plasma parameters differed from experimental values. The cause of this discrepancy is partially attributed to ‘spikes’ that occur within the plasma potential field, the origins of which are still not clear, and may be due to numerical instabilities. Also, it is noted that the duration of the simulations carried out so far are for ~ 2 microseconds – too short to capture the usually strong breathing mode that is typically in the 10-25 kHz range. This short computational time may also be too short to reach quasi-steady state – an issue that requires further examination.

II. Numerical Model

The 2D ($z - \theta$) cylindrical coordinate system is used in the simulation. First, we construct the simplest description able to treat electron transport self-consistently. In particular, the new description must resolve the inhomogeneous Hall current and the associated azimuthal fluctuations. As mentioned above, azimuthal waves have been seen experimentally in a number of Hall thrusters. Their amplitude is large and their power spectrum is complex, with coherent structures among random, broadband turbulence. Linear stability analyses have predicted

azimuthal unstable waves at low frequency (a few hundred kilohertz) and at high frequency (megahertz), driven unstable by resistivity and equilibrium gradients in plasma density and magnetic field.¹³ A nonlinear theory describing this cross-field transport mechanism is presently absent, except under simplifying assumptions. An example is the theory of Yoshikawa and Rose,¹⁴ which predicts a Bohm scaling for the electron transport with a coefficient proportional to the relative electron density fluctuation power. An objective of the model presented in this paper is to gain some understanding about the azimuthal fluctuations and their associated transport.

The $z - \theta$ model draws from our experience with the $z - r$ model. The main differences in the $z - \theta$ model come from the electron fluid description. The equations governing the electron fluid are current continuity, perpendicular momentum balance, and parallel momentum balance. The system is closed with an equation for the electric field and quasi-neutrality. For the results presented here, it is assumed that the magnetic field is purely radial (obtained from experiments), and does not vary with azimuthal position. The electron temperature is assumed to be constant in the azimuth direction and its axial variation is specified in accordance with that measured experimentally. This latter assumption is particularly severe. We make it at this point in order to simplify the system. As we begin to get results and better understand the model, a time-dependent electron energy equation that includes ionization, joule heating, wall damping (including sheath saturation¹⁵), and conductive and convective fluxes will be implemented. In time, the former assumption about the azimuthal symmetry of the magnetic field will also be relaxed, as it is found that axial asymmetry in the magnetic field appears to mode-lock lower frequency oscillations to the configuration of the magnetic poles.¹⁶ With these assumptions the electron fluid equations become:

$$\nabla \cdot (n_e \mathbf{u}_e - n_i \mathbf{v}_i) = 0 \quad (2)$$

$$u_{ez} = -\mu_\perp E_z - \frac{D_\perp}{n_e} \frac{\partial n_e}{\partial z} - \frac{1}{1 + (\nu/\omega_c)^2} \frac{E_\theta}{B} - \frac{1}{1 + (\nu/\omega_c)^2} \frac{kT_e}{en_e Br} \frac{\partial n_e}{\partial \theta} \quad (3)$$

$$u_{e\theta} = -\mu_\perp E_\theta - \frac{D_\perp}{n_e} \frac{\partial n_e}{\partial \theta} - \frac{1}{1 + (\nu/\omega_c)^2} \frac{E_z}{B} + \frac{1}{1 + (\nu/\omega_c)^2} \frac{kT_e}{en_e B} \frac{\partial n_e}{\partial z} \quad (4)$$

$$\phi = \frac{kT_e}{e} \ln n_e + \phi^* \quad (5)$$

$$\mathbf{E} = -\nabla \phi \quad (6)$$

$$n_e = n_i \quad (7)$$

Here, u_{ez} is the axial electron velocity, $u_{e\theta}$ is the azimuthal electron velocity, μ_\perp is the classical perpendicular mobility, ν is the electron-neutral collision frequency, ω_c is the electron cyclotron frequency, and D_\perp is the classical diffusion coefficient arising from electron-neutral collisions. The last four quantities are given by:

$$\mu_\perp = \frac{e/m_e \nu}{1 + (\nu/\omega_c)^2} \quad (8)$$

$$\nu = n_n \sigma_{en} \bar{c}_e \quad (9)$$

$$\omega_c = \frac{eB}{m_e} \quad (10)$$

$$D_\perp = \mu_\perp \frac{kT}{e} \quad (11)$$

In Eq. 9, $\sigma_{en} = 27 \times 10^{-20} \text{ m}^2$ is the electron-neutral elastic collision cross section, c_e is the mean electron speed (assuming a Maxwellian distribution), and m_e is the electron mass. In writing Eq. 2, we neglect transient space

charge accumulation. We note that the axial electron momentum equation (Eq. 3) now has components involving E_θ and $\partial n_e / \partial \theta$. These terms are proportional to $[1 + (\nu/\omega_c)^2]^{-1}$ and thus they are important at low neutral densities and high magnetic fields. We expect these terms to dominate near the exit of the channel, where ionization depletes the neutral concentration and the magnetic field is strongest. In the opposite limit, at high neutral densities and low magnetic fields characteristic of the anode region, these terms are expected to be small. The azimuthal electron momentum equation (Eq. 4) is absent in the $z - r$ models and it is an integral part of the current model. In high magnetic field and low neutral density regions, $u_{e\theta}$ is dominated by $\mathbf{E} \times \mathbf{B}$ and diamagnetic drifts, i.e., the third and fourth terms of Eq. 4 respectively. As before, the electric field \mathbf{E} (Eq. 6) is purely electrostatic and the parallel (radial) electron momentum equation (Eq. 5) results in a Boltzmann relation when integrated, defining the “thermalized potential,” ϕ^* . Quasi-neutrality (Eq. 7) closes the system, with n_i obtained from the ion particles via the PIC method. The solution of the equations above yields the electric field and electron fluid velocities. Bilinear interpolation of ion particle positions gives, by quasi-neutrality, the plasma density. The axial electron current $n_e u_{ez}$ is then obtained as well as an effective mobility. This mobility can be compared with the “classical” value and an assessment of fluctuation-induced transport can be made.

The treatment of the ions and the neutrals follows that of the $z - r$ model. Particle injection is done by inverting a Maxwellian flux distribution function.¹⁷ The nonlinear ionization rate is given by a fit to experiment according to the formula proposed by Ahedo et al.,¹⁸

$$\dot{n}_e = n_e n_n 5 \times 10^{-20} \sqrt{\frac{8kT_e}{\pi m_e}} \left(1 + \frac{T_e \varepsilon_I}{(T_e + \varepsilon_I)^2} \right) \exp(-\varepsilon_I / kT_e) \quad (12)$$

The geometry used in the simulation corresponds to that of the Stanford Hall Thruster (SHT), with a channel length of approximately 8 cm, and a circumference of approximately 34 cm. The computational domain extends from $z = 0$ (anode) to $z = 12$ cm (4 cm past the channel exit). A uniform rectangular grid in z and θ is used with 51 \times 50 grid points.

The boundary conditions for the electric potential in the axial coordinate are Dirichlet at the anode, where the anode potential is set at the discharge voltage ($\phi_{\text{anode}} = \phi_{\text{discharge}}$). A Dirichlet condition is also applied at the downstream boundary, where the potential is set to zero ($\phi_{\text{exit}} = 0$). In the azimuthal direction the boundary condition is periodic. Details of the discretization of the electron fluid equations and second-order finite difference technique used can be found in the paper by Fernandez et al.¹⁹ Reference 19 also presents details on the advancement of the particles using the PIC method. Here, we shall only briefly outline the solution procedure. Upon discretization of the equations and application of the boundary conditions, the resulting system becomes block-tridiagonal. The solution is found via a direct-solve method. The time step size for the iteration on the electron fluid equations is computed using the stability requirement⁵ that it be less than the electron plasma frequency $\omega_{pe} = \sqrt{n_e e^2 / m \varepsilon_0}$. The electric potential and electric field components then follow from Eqs. 5 and 6. Once the electric field is obtained, the particles are advanced (neutrals by their own inertia, ions in accordance with the local field), neutrals are ionized and ions born via a Monte Carlo method, neutrals are injected at the anode according to the given mass flow rate, and new particle densities are obtained with the PIC method. The electric potential is then found again and the cycle begins again. This process is shown schematically in Fig. 3. Note that the time advancement of the neutrals and ions is over some large number of time-steps used in the iteration on the electron fluid equations.

The neutral particles are assumed to reflect diffusely from all solid surfaces within the Hall thruster, including the anode. When the neutral (or ion) particles cross the cathode boundary they are removed from the simulation. When an ion interacts with a solid boundary it is assumed to undergo electron capture and become a neutral particle that is emitted diffusely at the wall temperature.

III. Results and Discussion

A typical simulation is initialized with a background of ions and neutrals placed uniformly in the domain. Their velocities are obtained by inverting a Maxwellian distribution function. A key parameter in the simulation is the value of the Hall parameter, ω_c/v . If this parameter has a small initial value, due for instance to a large value of n_n ,

the electron transport is found to be classical and azimuthal disturbances negligible. The electric field is localized axially to the region where the magnetic field is strongest and the azimuthal electric field is very small. Simulations that use uniform profiles for the magnetic field and electron temperature yield a uniform profile for the axial electric field, as expected. However, a simulation started with a small value of the Hall parameter does not remain with that small value except near the anode where the magnetic field is low and the neutral density is high. This is due to ionization, which eventually depletes the large initial neutral density and raises the value of the Hall parameter. Azimuthal fluctuations then emerge, along with their associated transport. An azimuthal electron velocity develops as shown in the $u_{e\theta}$ field rendering in Fig. 4, which is at a time of 1 μ s into a calculation, where the peak magnetic field is 50G, and the voltage is 150V. It is apparent in the figure that the

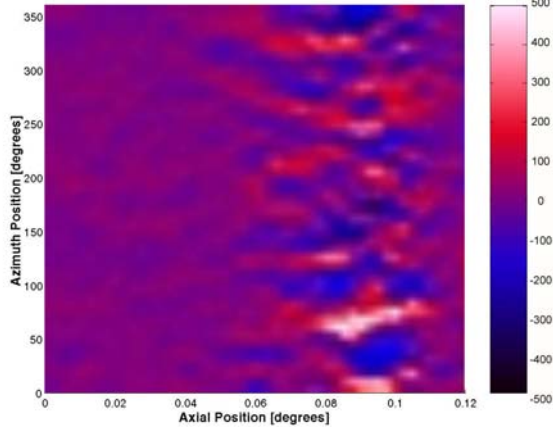


Figure 4. Field rendering of the computed azimuthal electron velocity.

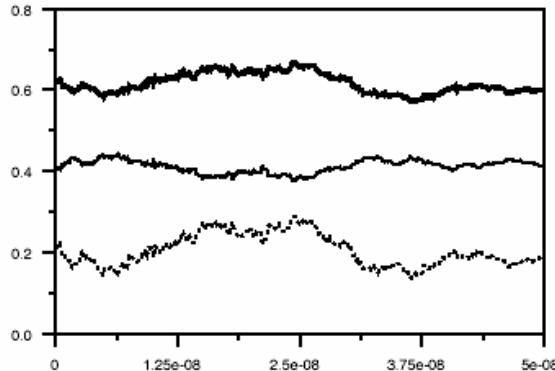


Figure 5: Electron current (amps) as a function of time (secs) The bold trace, solid trace and dashed trace represent the total current, the classical contribution, and the azimuthal fluctuation-induced contribution respectively.

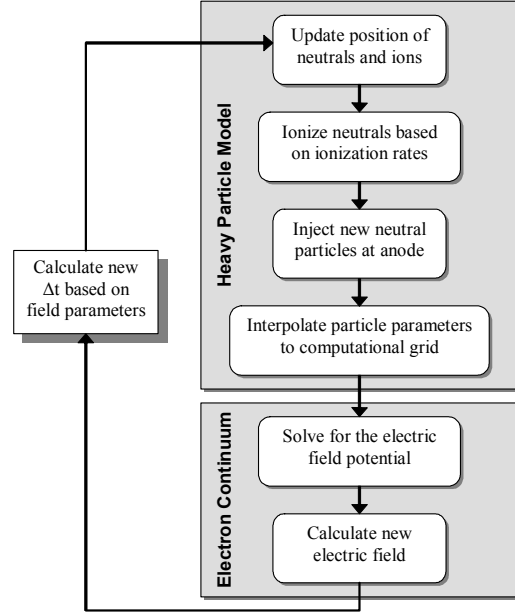


Figure 3: Flow chart for the numerical simulations

strongest fluctuations in the azimuthal velocity are near the region of maximum magnetic field. It also seems as though there is a coherent structure to these fluctuations, although a quantitative assessment of these oscillations is not yet complete. The classical and anomalous contributions to electron transport (where here anomalous is taken to be the transport associated with the last two azimuthal terms of Eq. 3), are shown in Fig. 5. It seems that the azimuthal contributions are indeed important, although numerical anomalies (see discussion below) prevent us from making definitive statements about cross-field transport due to correlated fluctuations at this time.

In order to better understand the predictive capability and behavior of the $z - \theta$ code, calculations were performed for cases corresponding to discharge conditions for which we have considerable experimental data.⁸ The majority of the results presented here are for a 100 G peak magnetic field, a mass flow rate of 2 mg/s through the 9 cm (inner diameter) channel approximately 1.2 cm in width. The simulated discharge time for each case was 1 - 2 μ s. While this time may be too small to reach the quasi steady state operating conditions of the thruster, it does provide partial insight into how well the simulation captures the structure of the discharge. It is noteworthy that a typical run takes an average of two weeks to compute on a single processor (Pentium 4) 3.0 GHz machine with 1 Gigabyte of RAM running in a Windows XP environment.

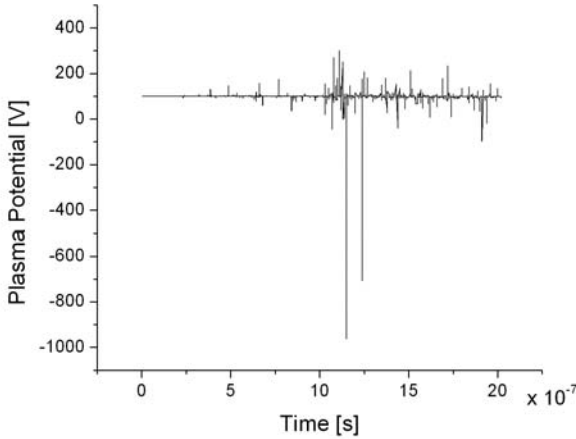


Figure 6: Temporal behavior of plasma potential.

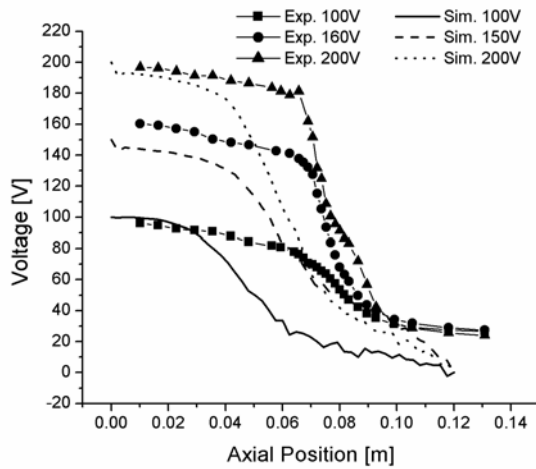


Figure 7: Comparison between measured and predicted (filtered) plasma potential.

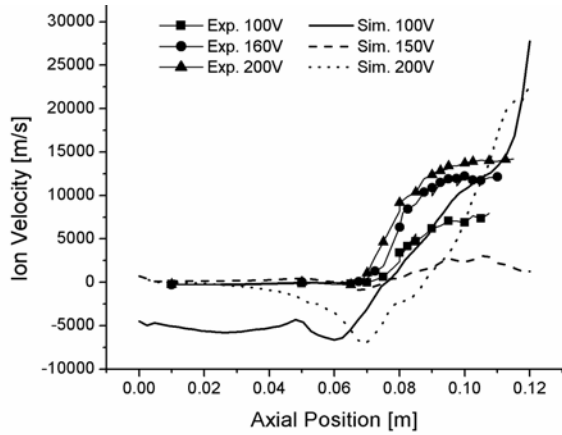


Figure 8: Comparison between measured and predicted (filtered) plasma potential.

A simple time averaging of the potential field over the duration of the simulation was carried out for comparison to the time-averaged potential measured within the discharge channel. This time averaging of the simulated potential field was found to give unphysical results (unusually large spatial oscillations), most notably in the region of the cathode plane. An examination of the data revealed that this was caused by strong spikes (of order the iterative time scale) in the plasma potential field. Figure 6 is an illustrative example of the temporal history of the plasma potential at the discharge exit. While over much of the computational time, the potential was well-behaved (at about ~ 100 V for this example), the temporal (positive and negative) spikes in the potential are apparent. In some cases, these fluctuations would become so large that the simulation would become numerically unstable. A filtering technique was implemented on the results which were stable, to exclude the effect of these fluctuations. The resulting comparison between measured and simulated (but filtered) plasma potential is depicted in Fig. 7. It can be observed from this figure that the simulation predicts the plasma potential reasonably well throughout the length of the acceleration channel. While the agreement between measurements and predictions is encouraging, this agreement may be somewhat fortuitous, in light of the required filtering and the appearance of these temporal anomalies in the data at very high frequencies, and the results are still rather unsettling.

The particle-averaged/time-averaged axial ion velocity predicted by the simulation is compared to experimental measurements in Fig. 8. The only conclusion that can be drawn at this time is that the simulation predicts acceleration where we expect it to be, and that the magnitude of this acceleration is comparable to that seen experimentally. However, one notable feature exists that is not seen (at least to this extent) in the simulations is that higher voltage operation predicts a substantial ion back-flow in the mid-channel location of the thruster. This negative ion velocity continues all the way to the anode in the case of the 200V discharge condition, contrary to what is seen experimentally. Since the model for the ion component of the simulation is purely kinetic and driven entirely by the gradients in the potential, and since the filtered potential variation shown in Fig. 6 is well-behaved, this unusual backflow is attributed to the ion response to the large unphysical fluctuations in potential, discussed above. It seems then that there are large bursts in ion velocity towards the anode, due to the strong fluctuations in the plasma potential.

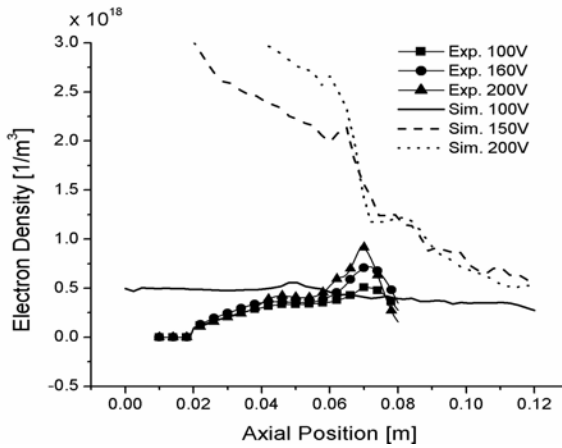


Figure 9: Comparison between measured and predicted plasma density.

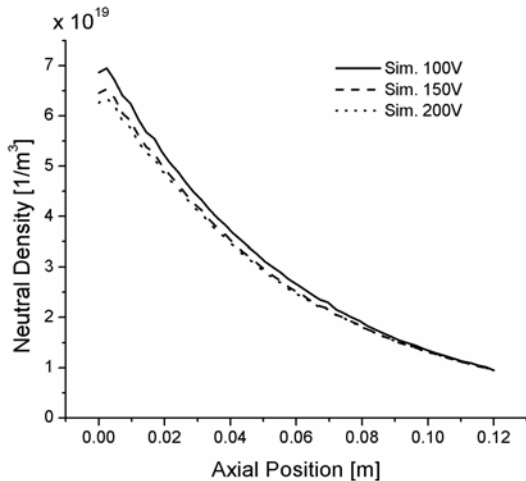


Figure 10: Predicted axial variation in the neutral particle density.

that accounts for the temperature-dependent secondary electron emission as well as sheath saturation effects. It is anticipated that adding the electron energy equation may serve to prevent the spikes seen in plasma potential. The method of solution must be refined and made more robust to run for $\sim 0.1 - 1$ msec. Over this time scale, the solution should capture the characteristic breathing modes seen experimentally at 15-20 kHz. An examination will also be made of the sensitivity of the solution to the overall grid structure.

Acknowledgements

M. Cappelli would like to acknowledge support from the Air Force Office of Scientific Research with Dr. Mitat Birkan as the program manager. E. Fernandez acknowledges the NASA/Stanford Center for Turbulence Research for partial support of this work.

The time-averaged simulated electron number density is compared to experimental values in Fig. 9. It is apparent that the simulations overpredict the plasma density throughout the channel, most notably near the anode. While ionization is partly driven by the high neutral density near the anode (see predictions of neutral density in Fig. 10), the electron temperature (which was imposed) in this region is low. The unexpected high plasma density near the anode may be partially connected to the strong negative flow of ions (toward the anode), which is a result of the potential spikes.

IV. Conclusions

We have investigated electron transport in Hall thrusters via numerical simulation using a hybrid fluid/PIC model in the $z - \theta$ coordinate space. At present, it represents a simplified description of Hall thruster plasmas but is able nonetheless to capture azimuthal flows, fluctuations, and their associated transport. Preliminary results indicate that for the typical large experimental values of the Hall parameters found in these engines, the electron transport associated with azimuthal disturbances is significant. However, numerical stability has prevented us from drawing any definitive conclusions at this time. In particular, the appearance of spurious spikes in the plasma potential at time scales associated with the iterative time step gives rise to unphysical ion velocities, and plasma density. The filtering of these spikes from the solution leads to plasma potential and velocity profiles that are at best in qualitative agreement with measurements.

Future work with the $z - \theta$ model lies in improving the numerical stability of the method of solution, and then subsequently examining the azimuthal fluctuations and transport in detail. The theory will be expanded by adding the electron energy equation to determine the spatial variation in the electron temperature. This equation should include a realistic wall damping model

References

- ¹F. Gulczinski, R. Spores, "Analysis of Hall Effect Thrusters and Ion Engines for Orbit Transfer Missions," AIAA-96-2973, 32nd Joint Propulsion Conference, Lake Buena Vista, FL (1996)
- ²A. Morozov, Y. Esipchuk, G. Tilinin, A. Trofimov, Y. Sharov, G. Shchepkin, "Plasma Accelerator with Closed Electron Drift and Extended Acceleration Zone," Sov. Phys. Tech. Phys. Vol. 17, pp. 38-45 (1972)
- ³E. Fernandez, M. A. Cappelli, K. Mahesh, "2D simulations of Hall thrusters," CTR Annual Research Briefs, pp. 81-91 (1998)
- ⁴M. Hirakawa, IEPC-97-67, 25th International Electric Propulsion Conference, Worthington, OH, (1997)
- ⁵J. C. Adam, A. Heron, G. Laval, "Study of stationary plasma thrusters using two-dimensional fully kinetic simulations," Phys. Plasmas Vol. 11, pp. 295-305, (2004)
- ⁶G. Janes, R. Lowder, "Anomalous Electron Diffusion and Ion Acceleration in a Low Density Plasma," Phys. Fluids Vol. 9, pp. 1115-1123., (1966)
- ⁷J. Bareilles, G.J.M. Hagelaar, L. Garrigues, C. Boniface, J.P. Boeuf, N. Gascon, "Critical assessment of a two-dimensional hybrid Hall thruster model: Comparisons with experiments," Phys. Plasmas, Vol. 11, pp. 3035-3046 (2004)
- ⁸B. Meezan, W. A. Hargus, Jr., and M. A. Cappelli, "Anomalous electron mobility in a coaxial Hall discharge plasma", Physical Review E., Volume 63, 026410 (2001)
- ⁹M. K. Allis, N. Gascon, C. Vialard_Goudou, M. A.Cappelli, E. Fernandez, "A comparison of hybrid Hall thruster model to experimental measurements," AIAA-2004-3951, 40th Joint Propulsion Conference, Ft. Lauderdale, FL (2004).
- ¹⁰E. Sommier, M.K. Allis, M.A. Cappelli, IEPC-2005-189, "Wall Erosion in 2D Hall Thruster Simulations" 29th International Electric Propulsion Conference, Princeton, NJ (2005)
- ¹¹J. M. Fife, *Hybrid-PIC Modeling and Electrostatic Probe Survey of Hall Thrusters*, Ph. D. Thesis: ¹¹.
- ¹²N. Gascon, private communication.
- ¹³E.Y. Choueiri, "Plasma oscillations in Hall thrusters," Phys. Plasmas Vol.8, pp. 1411-1426 (2001)
- ¹⁴. S. Yoshikawa, D. Rose, "Anomalous diffusion of a plasma across a magnetic field," Phys. Fluids, Vol.3, pp 334-340 (1962)
- ¹⁵S.Barral, K. Makowski, Z. Peradzynski, N. Gascon, M. Dudeck, "Wall material effects in stationary plasma thrusters: near-wall and in-wall conductivity," Phys. Plasmas Vol. 10, pp 4137-4152 (2003)
- ¹⁶E. Chesta, C. Lam, N.B. Meezan, D.P. Schmidt, M.A. Cappelli, "A Characterization of Plasma Fluctuations within a Hall Discharge," IEEE Transactions on Plasma Science Vol. 29, pp. 582-591 (2001)
Massachusetts Institute of Technology, Department of Aeronautics and Astronautics, September (1998)
- ¹⁷C.K.Birdsall, A.B. Langdon, "Plasma Physics via Computer Simulation," IOP Publishing Ltd. (1991)
- ¹⁸E. Ahedo, P. Martinez-Cerezo, M. Martinez-Sanchez, "One-dimensional model of the plasma flow in a Hall thruster," Phys. Plasmas, Vol. 8, pp. 3058-3068 (2001)
- ¹⁹E. Fernandez, M. Cappelli, N. Gascon, M. Allis, "Modeling Anomalous Electron Transport in Hall thrusters," CTR Annual Research Briefs (2004)